



Indole-substituted 2,4-diamino-5,8-dihydropyrido[2,3-*d*]pyrimidines from *one-pot* process and evaluation of their ability to bind dopamine receptors

Ricardo D. Enriz^a, Rodrigo D. Tosso^a, Sebastián A. Andújar^a, Nuria Cabedo^b,
Diego Cortés^b, Manuel Noguerras^c, Justo Cobo^c, Didier F. Vargas^d, Jorge Trilleras^{d,*}

^a IMIBIO-SL, CONICET, Facultad de Química Bioquímica y Farmacia, UNSL, San Luis, 5700, Argentina

^b Departamento de Farmacología, Laboratorio de Farmacoquímica, Facultad de Farmacia, Universidad de Valencia, Valencia, 46100, Spain

^c Departamento de Química Inorgánica y Orgánica, Universidad de Jaén, 23071, Jaén, Spain

^d Grupo de Investigación en Compuestos Heterocíclicos, Programa de Química, Facultad de Ciencias Básicas, Universidad del Atlántico, Puerto Colombia, 81007, Atlántico, Colombia

ARTICLE INFO

Article history:

Received 14 July 2018

Received in revised form

6 October 2018

Accepted 16 October 2018

Available online 18 October 2018

Keywords:

Pyridopyrimidine

Three-component synthesis

Bind dopamine

D1 and D2 receptors

Molecular modeling

ABSTRACT

A series of novel 7-indole substituted 2,4-diamino-5,8-dihydropyrido[2,3-*d*]pyrimidine analogous to the 2,4-diaminopteridine core were synthesized by the three-component *one-pot* cyclocondensation between 2,4,6-triaminopyrimidine, 3-(2-cyanoacetyl)indole and aromatic aldehydes. The reactions, which exhibited good performance, proceeded in EtOH using indium (III) chloride as catalyst under microwave irradiation, in short reaction times. On the basis of certain structural similarity of these compounds with known ligands of the D2 dopamine receptors (D2DR), the study of these compounds as possible ligands of dopamine D2 and D1 receptors was carried out. Three of them showed moderate affinity to D2-DR since the K_i D1/D2 ratio reached values of 40, 65 and 31 for compounds **4c**, **4k** and **4j**, respectively. Finally, molecular modeling studies revealed stronger molecular interactions of such derivatives with the D2DR than with D1DR, what agrees with the experimental data, and gives an additional support to the observed selectivity to the D2DR.

© 2018 Elsevier Ltd. All rights reserved.

1. Introduction

It is well known that a considerable number of pharmacologically relevant drugs contain nitrogen heterocyclic cores. For this reason the synthesis of heterocyclic systems, in parallel to the construction of molecular blocks that exhibit a great range of biological properties, has acquired an important role in the scientific community, especially in drug discovery field [1,2]. On the one hand, heterocyclic structures containing dihydropyrido[2,3-*d*]pyrimidine scaffolds have shown outstanding performances as anti-leishmanial agents [3], anti-inflammatory [4], antifungal [5], antiproliferative [6,7] and, more specifically, as antitumor agents [8–11]. Over the years, the number of publications concerning the pyridopyrimidine ring system has gradually increased [12,13]. Furthermore, new methodologies and strategies have been approached for their preparation; among them, microwave-

assistance [14–19], multicomponent processes (MCPs) [20–23] and catalytic methods [24–27] have acquired a prominent place.

The oxidized derivatives of dihydropyrido[2,3-*d*]pyrimidine have been described as 5-deaza-analogues of the pyrazino[2,3-*d*]pyrimidine core present in pterin, or in other important biological metabolites such folic acid and its antimetabolite methotrexate (Fig. 1a). Some deazapteridine analogues have also displayed relevant enzymatic activities, for example trimetrexate and piritrexim are dihydrofolate reductase (DHFR) inhibitors, and therefore they have been used as non-classical antifolate-drugs in the cancer treatment (Fig. 1b) [28–35]. In relation with this, we have already reported a new series of fused pyrimidine compounds with inhibitory effect on DHFR [36–38] and more recently another series acting as new inhibitors of BACE1 [39].

Regarding to a synthetic point of view, 3-cyanoacetylindole has been found to be a versatile building block for the synthesis of 3-substituted indole derivatives [40–43]. We have previously reported the use of this valuable precursor in the preparation of pyrido[2,3-*d*]pyrimidones *via* multicomponent *Knoevenagel* reactions [17,20]. The indole system is also a privileged medicinal

* Corresponding author.

E-mail address: jorgetrilleras@mail.uniatlantico.edu.co (J. Trilleras).

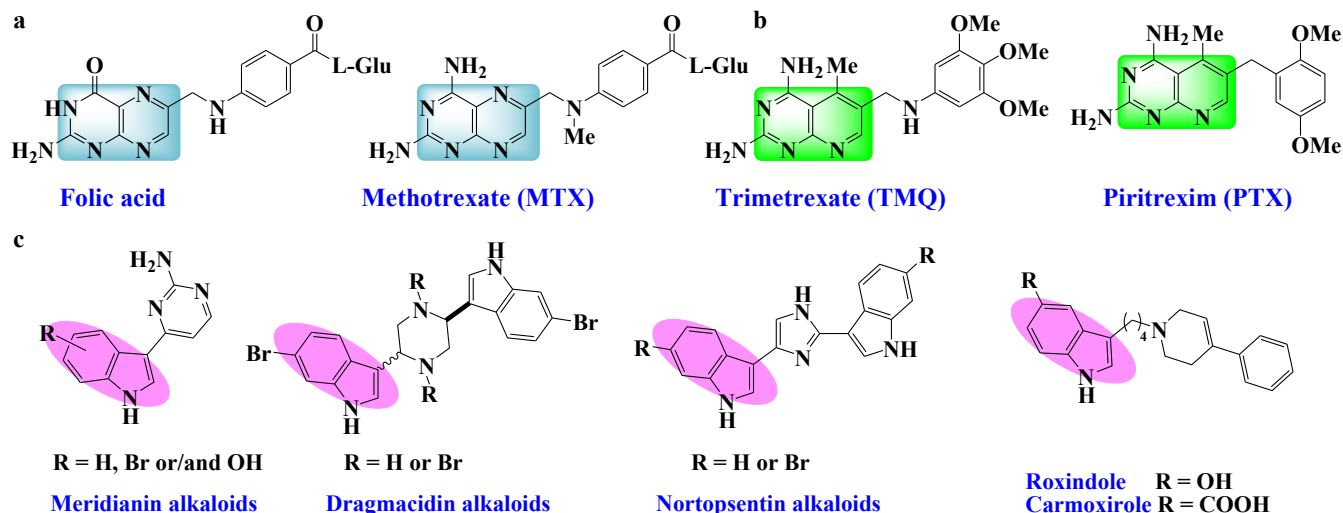


Fig. 1. (a) Examples of bioactive pteridines, (b) Deazapteridinic DHFR inhibitors, (c) 3-substituted indole derivatives.

scaffold, present in an interesting variety of pharmaceutical compounds as well as in bioactive marine natural occurring products. Some examples of the latter are the meridianins, monoindolic alkaloids [44], as well as bisindolic products dragmacidins [45,46] and nortopsentins [47] (Fig. 1c). These indole derivatives have shown *in vitro* cytotoxicity against a range of cancer cell lines. In addition, the indole core is found in some drugs used for fighting against central nervous system diseases, like roxindole, a dopaminergic agent and a potent 5-HT_{1A} receptor agonist [48,49].

Performing multicomponent reactions (MCRs) to afford molecular hybrids conforms with the perfect play in the design of new pharmacological entities necessary for searching treatments for a range of diseases. DHFR inhibitors containing the 2,4-diaminopyrimidine scaffold have been the target for the synthesis of new 2,4-diamino-pyrido[2,3-*d*]pyrimidine compounds which exhibit specific activities [29,34,50–54].

Moreover, we have reported different series of compounds acting as ligands of D2 and D1 dopamine receptors (D2DR and D1DR). Among others we have previously reported benzyltetrahydroisoquinolines (BTHIQs) [55–57], protoberberines [58], isoquinolines with hexahydrocyclopenta[*ij*]isoquinolines [59] and more recently carbamates [60]. Taking into account some structural similarity between the compounds reported here and some of the compounds previously reported as ligands of the dopamine receptors, we have evaluated the possible affinity of these indole-substituted derivatives with the dopamine D1 and D2 receptors. It is interesting to remark that dopamine-mediated neurotransmission plays an important role in relevant psychiatric and neurological disorders. Nowadays, there is an enormous interest in the development of new dopamine receptors (DR) acting drugs as potential new targets for the treatment of schizophrenia or Parkinson's disease. From a therapeutic point of view, drugs acting at D2-like DR are more relevant than those interacting with D1-like DR62 and in

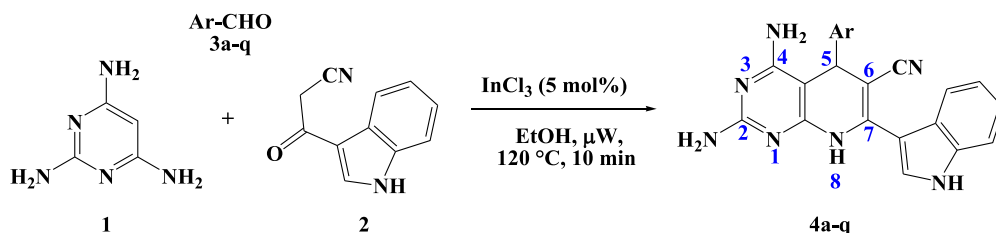
this sense more selective ligands are very welcome [61,62]. Finally, in order to assess the different molecular interactions that can stabilize or destabilize the distinct ligand-receptor (L-R) complexes in both receptor types, a molecular modeling study simulating the molecular interactions of the most characteristic ligands of each series with both D2 and D1 DR was carried out.

Based on the above precedents, and pursuing our interest in the synthesis of indole-substituted fused heterocycles [17,20], compounds that combine two pharmacophoric fragments, herein we disclose the synthesis of a series of 7-indole-substituted 2,4-diamino-5,8-dihydropyrido[2,3-*d*]pyrimidine hybrids **4** by the reaction of 2,4,6-triaminopyrimidine **1**, 3-(2-cyanoacetyl)indole **2** and aromatic aldehydes **3** as key components. The synthesis was carried out in an *one-pot* three-component reaction protocol under microwave irradiation assistance and InCl₃ catalysis, as shown in Scheme 1. The highlight advantages of combining multicomponent reactions (MCRs) with generation of molecular hybrids, are concerning to reaction rates, bond forming efficiency, simplicity and environmentally friendly properties, as well as, low costs if comparing to previous reported works [63–68].

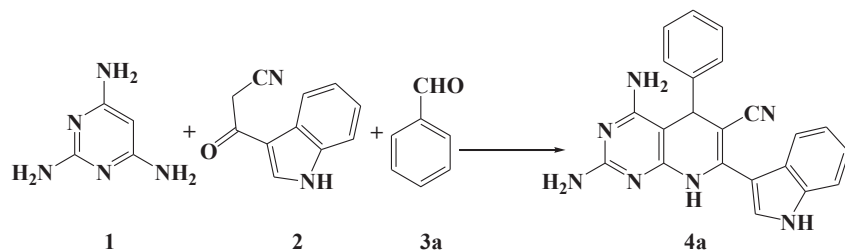
2. Results and discussion

2.1. Synthesis

Preliminary experiments for the cyclocondensation reaction were performed with benzaldehyde **3a** as model aldehyde (Table 1), using either commercially available or readily available starting materials under mild and low environmental impact reaction conditions. To set up the optimal reaction conditions, the influence of the solvent and catalyst were tested, as well as the use of conventional heating (Method A) and microwave irradiation (MWI) (Method B).



Scheme 1. Indium (III)-catalyzed three-component synthesis of 7-indole-substituted 2,4-diamino-5,8-dihydropyrido[2,3-*d*]pyrimidines **4**.

Table 1Optimization of the three-component synthesis of 7-indole-substituted 2,4-diamino-5,8-dihydropyrido[2,3-d]pyrimidines **4a**.

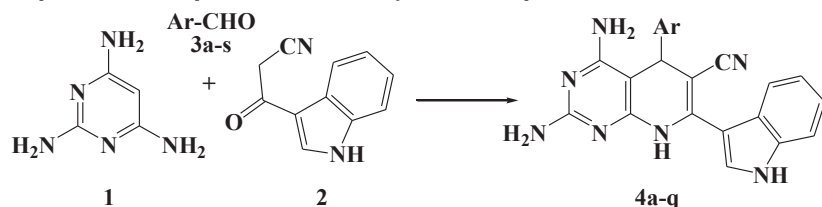
Entry	Conditions ^a		Method A		Method B	
	Solvent	InCl ₃ (mol%)	Yield (%) ^b	Time (hours)	Yield (%) ^b	Time (minutes)
1	AcOH	–	79	10	–	–
2	EtOH	5	75	3	86	10
3		10	70		84	
4		15	71		83	
5		Water	5		69	
6	Water	10	65	5	67	64
7		15	66		64	

^a 2,4,6-triaminopyrimidine **1** (1.0 equiv), 3-(2-cyanoacetyl)indole **2** (1.0 equiv) and benzaldehyde **3a** (1.0 equiv) dissolved in 5 mL of the respective solvent were used. Method A: The reaction was assisted by heating in an oil bath (conventional reflux). Method B: The reaction was assisted by microwave irradiation (μ W, 120 °C, 250 W, 250 PSI).

^b Yield of isolated product.

Following our recent reported procedure [20], the reaction was initially performed under conventional thermal conditions (Method A) using acetic acid as solvent. It was found that a precipitate appeared after 10 h under refluxing and isolated with 79% yield (entry 1). Reactions proceed similarly in the presence of InCl₃ as a catalyst [26,69]. This Lewis acid allows to use ethanol (entries 2–4) and water (entries 5–7) as eco-friendlier solvents. Under

these conditions, reaction times are reduced to 3 h being ethanol the appropriate solvent. To our delight, the use of MWI assistance for this transformation (Method B) exhibited an increase in yields of **4a** and the shorten in reaction time, only 10 min needed (Table 1, Method B, entries 2–4). In all cases the catalyst ratio (range 5–15%) was not a significant factor in the product yield, and the reaction gave a maximum yield of 86%, when it was carried out in EtOH

Table 2Scope of the multicomponent reaction for the synthesis of compounds **4**.

Entry	Product ^a	Aryl	Yield (%) ^c	Mp (°C)
1	4a	C ₆ H ₅	86	294–301
2	4b	4-Br-C ₆ H ₄	79	>300
3	4c	4-Cl-C ₆ H ₄	90	>300
4	4d	4-F-C ₆ H ₄	78	224–228
5	4e	3-F-C ₆ H ₄	75	194–199
6	4f	2-F-C ₆ H ₄	88	254–260
7	4g	4-CF ₃ -C ₆ H ₄	71	>300
8	4h	2-NO ₂ -C ₆ H ₄	77	285–289
9	4i	4-CH ₃ -C ₆ H ₄	88	>300
10	4j	3,4-di-OH-C ₆ H ₃	77	281–285
11	4k	4-CH ₃ O-C ₆ H ₄	78	>300
12	4l	3-CH ₃ O-C ₆ H ₄	76	>300
13	4m	2-CH ₃ O-C ₆ H ₄	70	301–303
Hetaryl				
14	4n	4-Pyridyl	78	260–264
15	4o	3-Pyridyl	87	>300
16	4p	2-Pyridyl	76	230–233
17	4q	2-Furanyl	70	>300
Knoevenagel adducts				
18	5r ^b	2,6-di-Cl-C ₆ H ₃	72	279–285
19	5s ^b	9-Anthracenyl	81	298–301

^a The reactions were carried out with 2,4,6-triaminopyrimidine **1** (1.0 equiv.), 3-(2-cyanoacetyl)indole **2** (1.0 equiv), benzaldehydes **3a-s** (1.0 equiv) and InCl₃ (5 mol%), in EtOH (5 mL), under microwaves irradiation (at 120 °C, 250 W, 250 PSI) for 10 min.

^b Knoevenagel condensation products **5r** and **5s**.

^c Isolated yields.

using only 5 mol% of InCl_3 (Table 1, Method B, entry 2).

In both conditions, method A and B, yields were higher using ethanol instead of water as solvent, in addition some reaction byproducts were observed by TLC but they were not isolated. The purpose of the trial, was to settle the reaction conditions to generate compound **4a** in a high-throughput manner.

Once the reaction conditions were established [5 mol% InCl_3 , EtOH, μW (120 °C, 250 W, 250 PSI), 10 min], the multicomponent process was successfully applied with different aromatic aldehydes (Table 2).

To evaluate the scope of this protocol regarding to aromatic aldehydes, electron-withdrawing (entries 2–8) and electron-donating (entries 9–13) groups as well as hetaryl aldehydes (entries 14–17) were tested, proceeding this *one-pot* three-component procedure quite well in any case, and efficiently giving the corresponding pyridopyrimidine-based molecules **4**. However, 2,6-dichlorobenzaldehyde (**3r**, entry 18) and 9-anthracenecarboxaldehyde (**3s**, entry 19) afforded only the respective *Knoevenagel* adducts and formation of 2,4-diamino-5,8-dihydropyrido[2,3-*d*]pyrimidine products was not observed. TLC monitoring of the reaction revealed that some aldehydes with electron-withdrawing groups were fully consumed in shorter reaction time (~7 min).

In general, the transformation culminated before 10 min of irradiation. The pyridopyrimidine-based molecules **4** were isolated as solids by simple filtration, purified by recrystallization from ethanol, and their structures were ascertained by IR, MS, NMR (^1H and ^{13}C) spectra and elemental analysis.

^1H NMR spectra of compounds **4a–q** exhibit characteristic signals for protons associated with heterocyclic rings. The signal to high field, a singlet at δ_{H} 4.71–5.30 ppm corresponding to C(5)H at dihydropyridinic ring. There are two singlets appearing at δ_{H} 5.68–6.13 ppm, each one integrating for 2 protons and corresponding to the amino groups at C(2) and C(4) in the pyrimidinic ring. Finally, two characteristic broad singlets appear at δ_{H} 9.21–9.49 and 11.62–11.70 ppm integrating each for 1 proton, which were assigned to the nitrogen endocyclic protons in the pyridinic and indolylic rings, respectively.

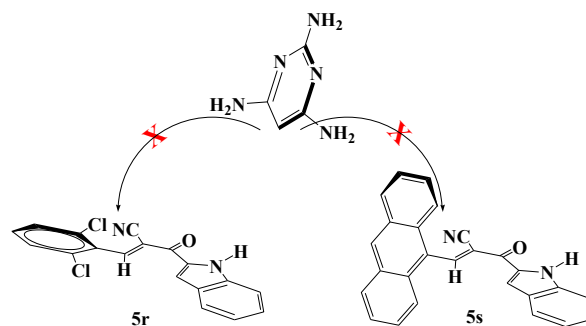
A mechanistic pathway has been proposed taking into account literature reports on the Lewis acid character and the chemistry of indium (III) compounds with different functional groups [26,69–72]. Therefore, as depicted from Scheme 2, the formation of the 7-indolyl-2,4-diamino-5,8-dihydropyrido[2,3-*d*]pyrimidine

derivatives **4** could be explained through three main stages. The first one is a *Knoevenagel* condensation between 3-cyanoacetylindole **2** and the aldehydes **3**, which is catalyzed by indium catalyst to form the adduct **A**, followed by *Michael* addition of 2,4,6-triaminopyrimidine **1** towards electron-deficient *Knoevenagel* adduct **A** to give the intermediate **B**.

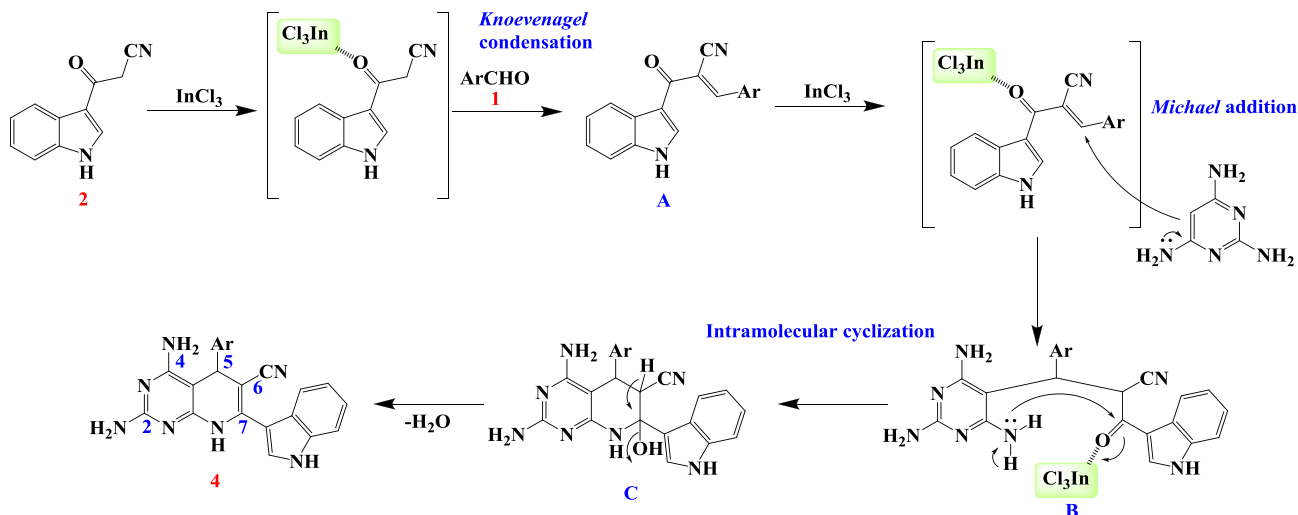
In turn, the latter can undergo intramolecular cyclization and subsequent dehydration to form products **4**. InCl_3 is likely to act as simple Lewis acid promoting each stage by coordination of In(III) with oxygen at carbonyl groups (Scheme 2).

TLC monitoring the reaction revealed a spot corresponding to *Knoevenagel* condensation product [**I**], which supports the mechanistic proposal. This spot ($R_f = 0.82$ in CH_2Cl_2 :EtOH 9:1) was observed during the whole process, until completion of the reaction. In previous reports, it was found that quenching the reaction before completion, a large part of *Knoevenagel* adducts was remained [17,20]. To our regrets, the increase of the reaction time to 30 min, under the same conditions of the reactants, did not afford satisfactory results for obtaining the **4r** and **4s** compounds, yet decomposition was observed.

The above fact supports the proposed mechanism because of the inability of aldehydes **3r** and **3s** to afford the respective pyridopyrimidines (Table 2, entries 18 and 19), giving only the corresponding *Knoevenagel* condensation products. In these specific cases, the *Michael* addition is strongly hindered and cannot take place due to the steric effects of the bulky substituents (Scheme 3), which preclude the approximation of the nucleophile, yielding only **5r** and **5s**.



Scheme 3. Adducts **5r** and **5s** containing bulky substituent.



Scheme 2. Plausible mechanism for the formation of **4**.

2.2. Binding affinities for dopamine receptors

Once the compounds were obtained, the second stage of our study was to evaluate their ability to bind dopamine D1 and D2 receptors. Three of the synthesized 7-indole-substituted 2,4-diamino-5,8-dihydropyrido[2,3-*d*]pyrimidine derivatives exhibited biological activity *in vitro* for their ability to displace the selective ligands of D1 and D2 DR from their respective specific binding sites in the striatal membranes (compounds **4c**, **4k** and **4j**). These compounds were able to displace [³H]-SCH 23390 and [³H]-raclopride from their specific binding sites at micromolar (μ M) concentrations. The binding affinities for D1 and D2 DR are summarized in Table 3 illustrating some general trends of the behavior of these compounds.

From the results shown in Table 3, it can be seen that the compounds reported here have a moderate affinity with both D1 and D2 receptors. An interesting result is that these compounds show a higher affinity for the D2 receptor compared to the D1 receptor. It should be noted that the K_i D1/D2 ratio reached values of 40, 65 and 31 for compounds **4c**, **4k** and **4j** respectively indicating their noticeable selectivity.

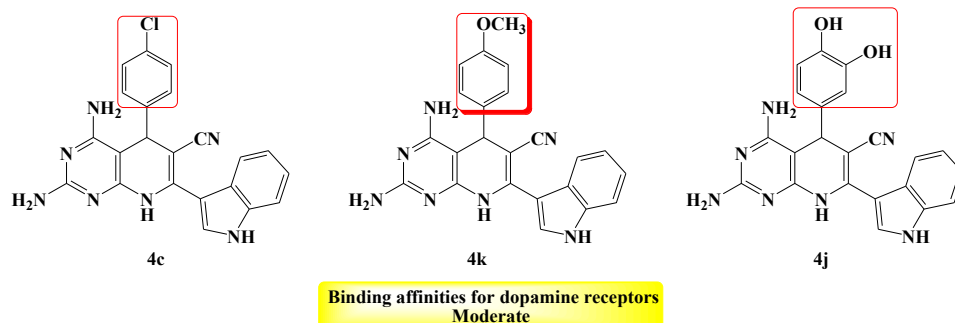
2.3. Molecular modeling

To better understand selectivity to D2-like DR, we performed a

molecular modeling study with compounds **4c**, **4k** and **4j**. We herein simulated the molecular interactions of these ligands with both receptors D1 and D2 to assess the different molecular interactions that can stabilize or destabilize the distinct L-R complexes. The molecular modeling study was conducted in three different stages. In the first step, a docking analysis was performed. In a second stage, molecular dynamics (MD) simulations were carried out and finally using the trajectories obtained from MD simulations, we performed an analysis per residue for the respective compounds.

In general, the three compounds displayed their pharmacophoric portions in a closely related spatial form to that reported for dopamine and other ligands [55–60]. Consistent with previous experimental [55–60] and theoretical [57,73] data, the simulation indicated the relevance of the negatively charged ASP78 and ASP74 for ligand binding in receptor D2DR and D1DR respectively. In this context, the highly conserved aspartate in trans-membrane helix 3 (TM3) may function as an anchoring point for ligands with protonated amino groups [55–60,73]. In the current study, all the compounds simulated were docked into the receptor with the protonated amino group close to aspartic group. Although after 10 ns of MD simulations the ligands slightly moved in a different way from the initial position, the strong interaction with ASP (78 for D2DR and 74 for D1DR) were maintained for all the complexes (see Fig. 2a and b), reinforcing the role of this amino acid as an

Table 3
Affinity values (K_i and pK_i) and selectivity ratios obtained for the active compounds.^a



Compound	Specific ligand D1 [³ H]-SCH 23390		Specific ligand D2 [³ H]-raclopride		K_i D1/D2
	K_i (μ M)	pK_i	K_i (μ M)	pK_i	
4c	69.59 \pm 2.35	4.157 \pm 0.117	1.748 \pm 0.172	5.757 \pm 0.054	40
4k	76.88 \pm 6.28	4.114 \pm 0.084	1.108 \pm 0.316	5.955 \pm 0.071	65
4j	66.34 \pm 5.33	4.178 \pm 0.104	2.169 \pm 0.654	5.664 \pm 0.077	31

^a Data were displayed as mean \pm SEM for 3 experiments. ANOVA, post Newmann-Keuls multiple comparison tests: ap < 0.05 vs D1-like dopaminergic receptor. bp < 0.01 vs D1-like dopaminergic receptor. cp < 0.001 vs D1-like dopaminergic receptor. dp < 0.001 vs **4c**. ep < 0.001 vs **4j**. fp < 0.01 vs **4k**.

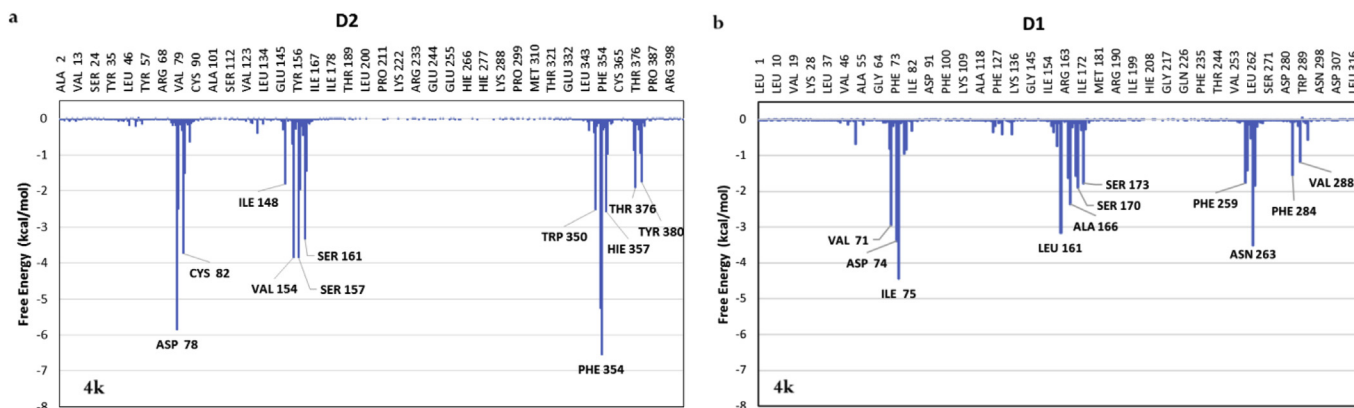


Fig. 2. Histograms showing the interaction energies of compound **4k** with the main amino acids involved in the complex formation. (a) D2DR and (b) D1DR.

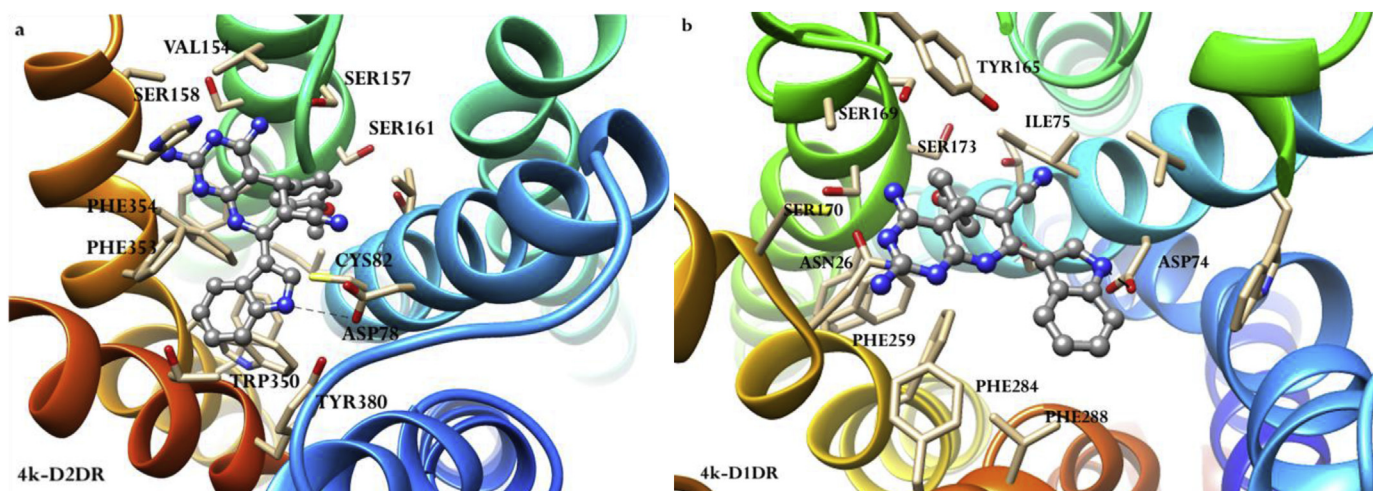


Fig. 3. Spatial view of compound **4k** interacting in the active sites of D2DR (a) and D1DR (b), respectively. The names of the residues involved in the main interactions are shown in this figure.

anchoring point for ligands with protonated amino groups.

To acquire more detailed insights into the mechanisms driving the binding of the pyridopyrimidine-based molecules to the active sites of D2DR and D1DR, the structure-affinity relationship was further analyzed. The residue interaction spectra calculated by the free energy decomposition for compounds **4c**, **4k** and **4j**, suggested that the interaction spectra with D2DR was closely related, and just only subtle differences were detected reflecting very similar binding features (compare Fig. 2a, Figs. 1Sa and 2Sa in supporting information).

However, there are appreciable differences when we compare the interactions obtained for these compounds with D1DR. For compound **4k**, the interaction obtained with ASP78 (D2DR) is stronger than that observed for ASP74 (D1DR) (Compare Fig. 2a and b). Another difference is the stronger interactions obtained for these compounds with the serine cluster (SER161 and SER157 in D2DR) with respect to the serine residues located at the D1DR (SER170 and SER173). There are numerous theoretical and experimental evidences [57–59,74] that demonstrate the importance of the role of the interactions with these serine residues for the stabilization of the complexes.

On the other hand, the hydrophobic interactions (TRP350, PHE353, PHE354, HIS357, TRP372 and TYR380) observed for **4c**, **4k** and **4j** at the D2DR are also stronger than those obtained in the D1DR (PHE259, ASN263, PHE284 and VAL288). These results indicate that, at least in part, the higher affinity of these compounds for D2DR with respect to D1DR could be due to these different interactions stabilizing the L-R complexes. These interactions are well observed in Fig. 3a and b for compound **4k** and Fig. 3Sa and 3Sb for compound **4c** (see supplementary material).

3. Conclusions

To sum up, we have developed a high-throughput *one-pot* multi-component process for the synthesis of a series of novel 7-indole-substituted 2,4-diamino-5,8-dihydropyrido[2,3-*d*]pyrimidine molecules. In addition, the combination of InCl_3 as promoter in EtOH and the microwave irradiation assistance provided an eco-friendly and attractive protocol towards this type of compounds. The reactions exhibited a broad scope, with tolerance to a wide variety of aromatic aldehydes, except those with bulky groups on both *ortho* positions respect to aldehyde function confirming this the proposed mechanism. Among this new series of compounds,

molecules **4c**, **4k** and **4j** showed a moderate affinity for both D2 and D1 dopamine receptors. A very interesting result from the point of view of medicinal chemistry is the selectivity shown by these compounds, by the receptor D2 with respect to D1. This is an interesting feature to carry out further studies on this type of structural scaffolding as potential dopaminergic agents.

On the other hand, the results obtained by our study of molecular modeling agree with the experimental data and provide us an explanation at molecular level about why these compounds show this preference for D2 dopamine receptors.

4. Experimental

4.1. General

Melting points (uncorrected) were determined with a Thermo scientific melting point apparatus, model IA 9100/Capillary. Infrared spectra (FT-IR) were collected at resolution of 2 cm^{-1} and 16 scans, (transmission mode $4000\text{--}500\text{ cm}^{-1}$) using a Shimadzu FTIR 8400 spectrophotometer (Scientific Instruments Inc., Seattle, WA, USA) and KBr disks. NMR spectra ^1H and ^{13}C (DEPT-135) were recorded on a Bruker Advance spectrophotometer operating at 400 and 100 MHz, respectively, using TMS as internal standard (δ , 0.0 ppm) and $\text{DMSO-}d_6$ as solvents. The NMR signals are reported in ppm and coupling constants (*J*) are reported in Hertz. Mass spectra were recorded in a Thermo Fisher Scientific GC-MS spectrometer model DSQII using a direct insertion probe and the electron impact ionization technique (70 eV). HRMS was recorded in an Agilent Technologies QTOF 6520B spectrometer coupled to a HPLC Agilent-1200 equipped with an Agilent Zorbax extend C18 ($2.1\text{ mm} \times 50\text{ mm} \times 1.8\text{ mm}$) PN 727700-902 column, via an electrospray ionization (ESI) and analyzed in a positive mode. HPLC method: 0.4 mL/min, gradient from acetonitrile/water (10%, with 0.1% of formic acid) to acetonitrile (with 0.1% of formic acid). The elemental analyses were obtained using a Thermo Finningan Flash EA11121 series elemental analyzer.

Microwave reactions were performed in borosilicate glass vessels (10 mL) using a focused microwave reactor (CEM Discover), which was adjusted to $120\text{ }^\circ\text{C}$ of target temperature and maximum power and pressure of 250 W, and 250 PSI respectively. TLC analyses were performed on silica gel aluminum plates (Merck 60 F₂₅₄) and spots visualized with a conventional UV lamp (254 or 365 nm). The ethanol and aromatic aldehydes **3a-s** were purchased from

commercial sources and used without further purification. Compounds 2,4,6-triaminopyrimidine **1** [75] and 3-(2-cyanoacetyl) indole **2** [17,76] were prepared according to reported procedures.

4.2. Synthesis of 2,4-diamino-5,8-dihydropyridopyrimidine-based hybrid molecules **4**

A mixture of 2,4,6-triaminopyrimidine **1** (1.0 mmol), 3-(2-cyanoacetyl)indole **2** (1.0 mmol), appropriate aromatic aldehyde (1.0 mmol) and indium chloride (0.05 mmol) in ethanol (5.0 mL) were subjected to microwave irradiation for 10 min at 120 °C. After completion of the reaction (monitored by TLC using a dichloromethane-ethanol (9:1) mixture as the mobile phase), the reaction mixture was cooled and filtered. The solid product obtained was initially washed with ethanol, and finally recrystallized from ethanol.

4.2.1. 2,4-Diamino-7-(1H-indol-3-yl)-5-phenyl-5,8-dihydropyrido[2,3-d]pyrimidine-6-carbonitrile (**4a**)

White solid; Yield: 86%; [Found: C, 69.7; H, 4.5; N, 25.9. C₂₂H₁₇N₇ requires C, 69.6; H, 4.5; N, 25.8%]; mp 294–301 °C; IR (KBr, cm⁻¹): 3494, 3427, 3392, 3280, 3120 (NH, NH₂), 2192 (C≡N), 1622 (C=N); d_H (400 MHz, DMSO-*d*₆) 4.78 (1H, s, H-5), 5.72 (2H, s, 2-NH₂), 6.00 (2H, s, 4-NH₂), 7.07 (1H, t, *J* 7.5 Hz, indolyl-H), 7.16 (1H, t, *J* 7.5 Hz, indolyl-H), 7.24 (1H, t, *J* 7.2 Hz, Ar-H), 7.34 (2H, t, *J* 7.5 Hz, Ar-H), 7.41 (2H, d, *J* 7.1 Hz, Ar-H), 7.43 (1H, d, *J* 7.6 Hz, indolyl-H), 7.46 (1H, d, *J* 8.1 Hz, indolyl-H), 7.73 (1H, d, *J* 2.4 Hz, indolyl-H), 9.32 (1H, s, 8-NH), 11.65 (1H, s, indolyl-NH); d_C (100 MHz DMSO-*d*₆) 38.6, 81.5, 85.6, 107.9, 112.0, 119.7, 119.8, 121.8, 125.1, 126.7, 127.0, 127.5, 128.4, 135.9, 145.1, 145.9, 154.6, 161.7, 161.9; *m/z* (rel. int. %): 379 (6, M⁺), 303 (20), 302 (100), 260 (11); HRMS (ESI-QTOF positive ionization): MH⁺ found 380.1615. C₂₂H₁₇N₇ requires 380.1618.

4.2.2. 2,4-Diamino-5-(4-bromophenyl)-7-(1H-indol-3-yl)-5,8-dihydropyrido[2,3-d]pyrimidine-6-carbonitrile (**4b**)

White solid; [Found: C, 57.7; H, 3.6; N, 21.4. C₂₂H₁₆BrN₇ requires C, 57.6; H, 3.5; N, 21.4%]; Yield: 79%; mp > 300 °C; IR (KBr, cm⁻¹): 3493, 3432, 3390, 3256, 3149 (NH, NH₂), 2203 (C≡N), 1629 (C=N); d_H (400 MHz, DMSO-*d*₆) 4.80 (1H, s, H-5), 5.75 (2H, s, 2-NH₂), 6.04 (2H, s, 4-NH₂), 7.09 (1H, t, *J* 7.4 Hz, indolyl-H), 7.17 (1H, t, *J* 7.5 Hz, indolyl-H), 7.35 (2H, d, *J* 8.3 Hz, Ar-H), 7.42 (1H, d, *J* 7.9 Hz, indolyl-H), 7.46 (1H, d, *J* 8.1 Hz, indolyl-H), 7.56 (2H, d, *J* 8.3 Hz, Ar-H), 7.73 (1H, d, *J* 2.4 Hz, indolyl-NH), 9.37 (1H, s, 8-NH), 11.66 (1H, s, indolyl-NH); d_C (100 MHz DMSO-*d*₆) 38.0, 80.9, 85.1, 107.7, 112.1, 119.8, 119.8, 121.7, 121.9, 125.1, 127.7, 129.2, 131.3, 135.9, 145.2, 145.3, 154.5, 161.8, 161.9; *m/z* (rel. int. %): 457 (2, M⁺), 303 (22), 302 (100), 260 (13); HRMS (ESI-QTOF positive ionization): MH⁺ found 458.072. C₂₂H₁₆BrN₇ requires 458.0723.

4.2.3. 2,4-Diamino-5-(4-chlorophenyl)-7-(1H-indol-3-yl)-5,8-dihydropyrido[2,3-d]pyrimidine-6-carbonitrile (**4c**)

Light yellow solid; [Found: C, 63.8; H, 4.0; N, 23.7. C₂₂H₁₆ClN₇ requires C, 63.9; H, 3.9; N, 23.7%]; Yield: 90%; mp > 300 °C; IR (KBr, cm⁻¹): 3432, 3392, 3256, 3144 (NH, NH₂), 2203 (C≡N), 1632 (C=N); d_H (400 MHz, DMSO-*d*₆) 4.81 (1H, s, H-5), 5.74 (2H, s, 2-NH₂), 6.04 (2H, s, 4-NH₂), 7.08 (1H, t, *J* 7.5 Hz, indolyl-H), 7.16 (1H, t, *J* 7.5 Hz, indolyl-H), 7.39–7.46 (6H, m, 4H Ar-H + 2H indolyl-H), 7.73 (1H, d, *J* 2.4 Hz, indolyl-H), 9.37 (1H, s, 8-NH), 11.66 (1H, s, indolyl-NH); d_C (100 MHz DMSO-*d*₆) 37.9, 80.9, 85.2, 107.6, 112.0, 119.8, 119.8, 121.7, 121.9, 125.1, 127.7, 128.4, 128.8, 131.3, 135.9, 144.8, 145.3, 154.5, 161.8, 161.9; *m/z* (rel. int. %): 413 (5, M⁺), 303 (20), 302 (100),

260 (11); HRMS (ESI-QTOF positive ionization): MH⁺ found 414.1226. C₂₂H₁₆ClN₇ requires 414.1228.

4.2.4. 2,4-Diamino-5-(4-fluorophenyl)-7-(1H-indol-3-yl)-5,8-dihydropyrido[2,3-d]pyrimidine-6-carbonitrile (**4d**)

White solid; Yield: 78%; [Found: C, 66.5; H, 4.1; N, 24.7. C₂₂H₁₆FN₇ requires C, 66.5; H, 4.1; N, 24.7%]; mp 224–228; IR (KBr, cm⁻¹): 3491, 3359, 3143 (NH, NH₂), 2193 (C≡N), 1634 (C=N); d_H (400 MHz, DMSO-*d*₆) 4.81 (1H, s, H-5), 5.74 (2H, s, 2-NH₂), 6.03 (2H, s, 4-NH₂), 7.08 (1H, t, *J* 7.5 Hz, indolyl-H), 7.14–7.20 (3H, m, Ar-H + indolyl-H), 7.41–7.44 (3H, m, Ar-H + indolyl-H), 7.46 (1H, d, *J* 8.1 Hz, indolyl-H), 7.73 (1H, d, *J* 2.5 Hz, indolyl-H), 9.35 (1H, s, 8-NH), 11.66 (1H, s, indolyl-NH); d_C (100 MHz DMSO-*d*₆) 37.8, 81.4, 85.5, 107.8, 112.1, 115.2, 119.8, 119.8, 121.8, 121.9, 125.1, 127.7, 128.8, 135.9, 142.2, 145.1, 154.5, 161.1, 161.8, 161.9; *m/z* (rel. int. %): 397 (7, M⁺), 303 (20), 302 (100), 260 (12); HRMS (ESI-QTOF positive ionization): MH⁺ found 398.1524. C₂₂H₁₆FN₇ requires 398.1524.

4.2.5. 2,4-Diamino-5-(3-fluorophenyl)-7-(1H-indol-3-yl)-5,8-dihydropyrido[2,3-d]pyrimidine-6-carbonitrile (**4e**)

White solid; [Found: C, 66.5; H, 4.0; N, 24.7. C₂₂H₁₆FN₇ requires C, 66.5; H, 4.1; N, 24.7%]; Yield: 75%; mp 194–199 °C; IR (KBr, cm⁻¹): 3499, 3341, 3151 (NH, NH₂), 2197 (C≡N), 1666 (C=N); d_H (400 MHz, DMSO-*d*₆) 4.84 (1H, s, H-5), 5.77 (2H, s, 2-NH₂), 6.09 (2H, s, 4-NH₂), 7.08–7.11 (2H, m, Ar-H + indolyl-H), 7.15–7.19 (2H, m, Ar-H + indolyl-H), 7.25 (1H, d, *J* 7.8 Hz, Ar-H), 7.38–7.44 (2H, m, Ar-H + indolyl-H), 7.46 (1H, d, *J* 8.1 Hz, indolyl-H), 7.76 (1H, d, *J* 2.5 Hz, indolyl-H), 9.53 (1H, s, 8-NH), 11.68 (1H, s, indolyl-NH); d_C (100 MHz DMSO-*d*₆) 38.3, 80.7, 85.1, 107.7, 112.1, 113.5, 113.5, 119.8, 121.7, 121.9, 123.1, 125.1, 127.7, 130.5, 135.9, 145.5, 148.8, 154.6, 161.8, 161.9, 163.4; *m/z* (rel. int. %): 397 (6, M⁺), 303 (20), 302 (100), 260 (14); HRMS (ESI-QTOF positive ionization): MH⁺ found 398.1524. C₂₂H₁₆FN₇ requires 398.1524.

4.2.6. 2,4-Diamino-5-(2-fluorophenyl)-7-(1H-indol-3-yl)-5,8-dihydropyrido[2,3-d]pyrimidine-6-carbonitrile (**4f**)

White solid; [Found: C, 66.4; H, 4.1; N, 24.7. C₂₂H₁₆FN₇ requires C, 66.5; H, 4.1; N, 24.7%]; Yield: 88%; mp 254–260 °C; IR (KBr, cm⁻¹): 3501, 3430, 3381, 3204 (NH, NH₂), 2191 (C≡N), 1631 (C=N); d_H (400 MHz, DMSO-*d*₆) 5.03 (1H, s, H-5), 5.75 (2H, s, 2-NH₂), 5.81 (2H, s, 4-NH₂), 7.07 (1H, t, *J* 7.4 Hz, indolyl-H), 7.14–7.22 (3H, m, 2H Ar-H + indolyl-H), 7.30 (1H, t, Ar-H), 7.38–7.43 (2H, m, Ar-H + indolyl-H), 7.45 (1H, d, *J* 8.2 Hz, indolyl-H), 7.72 (1H, d, *J* 2.5 Hz, indolyl-H), 9.40 (1H, s, 8-NH), 11.64 (1H, s, indolyl-NH); d_C (100 MHz DMSO-*d*₆) 34.2, 79.5, 84.1, 107.8, 112.0, 115.8, 119.7, 119.8, 121.5, 121.8, 124.4, 125.1, 127.5, 128.9, 129.8, 131.6, 135.9, 145.9, 154.9, 159.0, 161.7, 161.9; *m/z* (rel. int. %): 397 (8, M⁺), 303 (23), 302 (100), 260 (14); HRMS (ESI-QTOF positive ionization): MH⁺ found 398.1520. C₂₂H₁₆FN₇ requires 398.1524.

4.2.7. 2,4-Diamino-7-(1H-indol-3-yl)-5-[4-(trifluoromethyl)phenyl]-5,8-dihydropyrido[2,3-d]pyrimidine-6-carbonitrile (**4g**)

White solid; [Found: C, 61.8; H, 3.6; N, 21.9. C₂₃H₁₆F₃N₇ requires C, 61.7; H, 3.6; N, 21.9%]; Yield: 71%; mp > 300 °C; IR (KBr, cm⁻¹): 3493, 3439, 3390, 3259, 3154 (NH, NH₂), 2206 (C≡N), 1630 (C=N); d_H (400 MHz, DMSO-*d*₆) 4.95 (1H, s, H-5), 5.81 (2H, s, 2-NH₂), 6.10 (2H, s, 4-NH₂), 7.09 (1H, t, *J* 7.1 Hz, indolyl-H), 7.17 (1H, t, *J* 7.2 Hz, indolyl-H), 7.44 (1H, d, *J* 8.4 Hz, indolyl-H), 7.47 (1H, d, *J* 8.4 Hz, indolyl-H), 7.62 (2H, d, *J* 7.5 Hz, Ar-H), 7.76 (3H, bb, 2H Ar-H + indolyl-H), 9.46 (1H, s, 8-NH), 11.69 (1H, s, indolyl-NH); d_C (100 MHz DMSO-*d*₆) 38.4, 80.5, 84.9, 107.7, 112.1, 119.8, 121.7, 121.9, 125.1, 125.5, 127.8, 136.0, 145.7, 150.3, 154.7, 161.9, 162.0; *m/z* (rel.

int. %): 447 (5, M⁺), 303 (20), 302 (100), 260 (12); HRMS (ESI-QTOF positive ionization): MH⁺ found 448.1497. C₂₃H₁₆F₃N₇ requires 448.1492.

4.2.8. 2,4-Diamino-7-(1H-indol-3-yl)-5-(2-nitrophenyl)-5,8-dihydropyrido[2,3-d]pyrimidine-6-carbonitrile (**4h**)

Yellow solid; [Found: C, 62.3; H, 3.8; N, 26.5. C₂₂H₁₆N₈O₂ requires C, 62.3; H, 3.8; N, 26.4%]; Yield: 77%; mp 285–289 °C; IR (KBr, cm⁻¹): 3282, 3087 (NH, NH₂), 2194 (C≡N), 1631 (C=N) cm⁻¹; d_H (400 MHz, DMSO-d₆) 5.30 (1H, s, H-5), 5.79 (2H, s, 2-NH₂), 5.88 (2H, s, 4-NH₂), 7.05 (1H, t, J 7.4 Hz, indolyl-H), 7.15 (1H, t, J 7.5 Hz, indolyl-H), 7.36 (1H, d, J 7.7 Hz, indolyl-H), 7.44 (1H, d, J 8.1 Hz, indolyl-H), 7.54 (1H, t, J 7.6 Hz, Ar-H), 7.60 (1H, d, J 8.0 Hz, Ar-H), 7.71 (1H, d, J 2.5 Hz, indolyl-H), 7.76 (1H, t, J 7.6 Hz, Ar-H), 7.90 (1H, d, J 8.0 Hz, Ar-H), 9.49 (1H, s, 8-NH), 11.65 (1H, s, indolyl-NH); d_C (100 MHz DMSO-d₆) 35.1, 80.9, 84.1, 107.5, 112.0, 119.7, 119.8, 120.8, 121.9, 123.8, 125.0, 127.7, 128.6, 130.9, 134.1, 135.9, 139.4, 145.4, 147.8, 155.0, 161.9, 162.1; m/z (rel. int. %): 376 (26), 375 (64), 374 (92), 65.9 (100); HRMS (ESI-QTOF positive ionization): MH⁺ found 425.1475. C₂₂H₁₆N₈O₂ requires 425.1469.

4.2.9. 2,4-Diamino-7-(1H-indol-3-yl)-5-(4-methylphenyl)-5,8-dihydropyrido[2,3-d]pyrimidine-6-carbonitrile (**4i**)

Yellow solid; [Found: C, 70.2; H, 4.9; N, 25.0. C₂₃H₁₉N₇ requires C, 70.2; H, 4.9; N, 24.9%]; Yield: 88%; mp > 300 °C; IR (KBr, cm⁻¹): 3473, 3433, 3357, 3219 (NH, NH₂), 2195 (C≡N), 1682 (C=N); d_H (400 MHz, DMSO-d₆) 2.28 (3H, s, Ar-CH₃), 4.72 (1H, s, H-5), 5.70 (2H, s, 2-NH₂), 5.95 (2H, s, 4-NH₂), 7.07 (1H, t, J 7.9 Hz, indolyl-H), 7.15 (2H, d, J 8.2 Hz, Ar-H), 7.16 (1H, t, J 7.5 Hz, indolyl-H), 7.28 (2H, d, J 8.2 Hz, Ar-H), 7.44 (2H, t, indolyl-H), 7.71 (1H, d, J 2.5 Hz, indolyl-H), 9.27 (1H, s, 8-NH), 11.63 (1H, s, indolyl-NH); d_C (100 MHz DMSO-d₆) 20.7, 38.3, 81.7, 85.8, 107.9, 112.0, 119.7, 119.9, 121.8, 125.1, 127.0, 127.5, 129.0, 135.8, 135.9, 143.0, 144.9, 154.4, 161.6, 161.9; m/z (rel. int. %): 393 (6, M⁺), 303 (23), 302 (100), 260 (14); HRMS (ESI-QTOF positive ionization): MH⁺ found 394.1772. C₂₃H₁₉N₇ requires 394.1775.

4.2.10. 2,4-Diamino-5-(3,4-dihydroxyphenyl)-7-(1H-indol-3-yl)-5,8-dihydropyrido[2,3-d]pyrimidine-6-carbonitrile (**4j**)

Orange solid; [Found: C, 64.2; H, 4.2; N, 23.9. C₂₂H₁₇N₇O₂ requires C, 64.2; H, 4.2; N, 23.8%]; Yield: 77%; mp 281–285 °C; IR (KBr, cm⁻¹): 3500–3100 (OH, NH, NH₂), 2210 (C≡N), 1654 (C=N); d_H (400 MHz, DMSO-d₆) 4.57 (1H, s, H-5), 5.68 (2H, s, 2-NH₂), 5.87 (2H, s, 4-NH₂), 6.43 (1H, s, Ar-OH), 6.68 (1H, s, Ar-H), 6.77 (1H, s, Ar-H), 7.08 (1H, t, J 7.5 Hz, indolyl-H), 7.16 (1H, t, J 7.7 Hz, indolyl-H), 7.45 (2H, d, J 8.4 Hz, indolyl-H), 7.70 (1H, d, J 2.1 Hz, indolyl-H), 8.82 (1H, s, Ar-OH), 9.21 (1H, s, 8-NH), 11.62 (1H, s, indolyl-NH); d_C (100 MHz DMSO-d₆) 38.1, 82.3, 86.0, 108.1, 112.0, 114.7, 115.2, 118.0, 119.7, 120.0, 121.8, 122.0, 125.2, 127.4, 135.9, 137.1, 144.2, 144.3, 145.2, 154.4, 161.6, 162.0; m/z (rel. int. %): 302 (33), 301 (58), 300 (27), 109.9 (100); HRMS (ESI-QTOF positive ionization): MH⁺ found 412.1518. C₂₂H₁₇N₇O₂ requires 412.1516.

4.2.11. 2,4-Diamino-7-(1H-indol-3-yl)-5-(4-methoxyphenyl)-5,8-dihydropyrido[2,3-d]pyrimidine-6-carbonitrile (**4k**)

White solid; [Found: C, 67.5; H, 4.6; N, 24.0. C₂₃H₁₉N₇O requires C, 67.5; H, 4.6; N, 23.9%]; Yield: 78%; mp > 300 °C; IR (KBr, cm⁻¹): 3491, 3357, 3143 (NH, NH₂), 2193 (C≡N), 1634 (C=N); d_H (400 MHz, DMSO-d₆) 3.74 (3H, s, Ar-OCH₃), 4.71 (1H, s, H-5), 5.70 (2H, s, 2-NH₂), 5.96 (2H, s, 4-NH₂), 6.91 (2H, d, J 8.6 Hz, Ar-H), 7.08 (1H, t, J 7.6 Hz, indolyl-H), 7.16 (1H, t, J 7.5 Hz, indolyl-H), 7.32 (2H, d, J 8.6 Hz, Ar-H), 7.44 (1H, d, J 7.7 Hz, indolyl-H), 7.72 (1H, d, J 2.5 Hz,

indolyl-H), 9.27 (1H, s, 8-NH), 11.63 (1H, s, indolyl-NH); d_C (100 MHz DMSO-d₆) 37.8, 55.0, 81.9, 85.9, 108.0, 112.0, 113.8, 119.7, 119.9, 121.8, 121.9, 125.1, 127.5, 128.1, 135.9, 138.2, 144.7, 154.4, 158.1, 161.6, 161.9; m/z (rel. int. %): 409 (8, M⁺), 303 (20), 302 (100), 260 (11); HRMS (ESI-QTOF positive ionization): MH⁺ found 410.1719. C₂₃H₁₉N₇O requires 410.1724.

4.2.12. 2,4-Diamino-7-(1H-indol-3-yl)-5-(3-methoxyphenyl)-5,8-dihydropyrido[2,3-d]pyrimidine-6-carbonitrile (**4l**)

Light yellow solid; [Found: C, 67.4; H, 4.6; N, 24.0. C₂₃H₁₉N₇O requires C, 67.5; H, 4.7; N, 23.9%]; Yield: 76%; m.p. > 300 °C; IR (KBr, cm⁻¹): 3480, 3463, 3436, 3367, 3160 (NH, NH₂), 2184 (C≡N), 1669 (C=N); d_H (400 MHz, DMSO-d₆) 3.74 (3H, s, Ar-OCH₃), 4.75 (1H, s, H-5), 5.74 (2H, s, 2-NH₂), 6.03 (2H, s, 4-NH₂), 6.82 (1H, d, J 8.3 Hz, Ar-H), 6.99 (1H, d, J 8.3 Hz, Ar-H), 7.00 (1H, s, Ar-H), 7.09 (1H, t, J 7.5 Hz, indolyl-H), 7.17 (1H, t, J 7.6 Hz, indolyl-H), 7.27 (1H, t, J = 7.8 Hz, Ar-H), 7.46 (1H, d, J 7.1 Hz, indolyl-H), 7.74 (1H, d, J 2.4 Hz, indolyl-H), 9.33 (1H, s, 8-NH), 11.66 (1H, s, indolyl-NH); d_C (100 MHz DMSO-d₆) 38.6, 55.0, 81.3, 85.6, 107.9, 111.5, 112.1, 113.4, 119.4, 119.8, 119.8, 121.9, 125.1, 127.6, 129.6, 135.9, 145.2, 147.5, 154.5, 159.3, 161.7, 161.9; m/z (rel. int. %): 409 (3, M⁺), 303 (20), 302 (100), 260 (11); HRMS (ESI-QTOF positive ionization): MH⁺ found 410.1722. C₂₃H₁₉N₇O requires 410.1724.

4.2.13. 2,4-Diamino-7-(1H-indol-3-yl)-5-(2-methoxyphenyl)-5,8-dihydropyrido[2,3-d]pyrimidine-6-carbonitrile (**4m**)

White solid; [Found: C, 67.5; H, 4.7; N, 23.9. C₂₃H₁₉N₇O requires C, 67.5; H, 4.7; N, 23.9%]; Yield: 70%; mp > 300 °C; IR (KBr, cm⁻¹): 3492, 3391, 3310, 3140 (NH, NH₂), 2197 (C≡N), 1638 (C=N); d_H (400 MHz, DMSO-d₆) 3.86 (3H, s, Ar-OCH₃), 4.99 (1H, s, H-5), 5.71 (4H, s, 2-NH₂ + 4-NH₂), 6.99 (1H, t, J 7.6 Hz, Ar-H), 7.06 (1H, d, J 7.6 Hz, Ar-H), 7.08 (1H, t, J 7.7 Hz, indolyl-H), 7.17 (1H, t, J 7.5 Hz, indolyl-H), 7.25 (1H, t, J 7.5 Hz, Ar-H), 7.34 (1H, d, J 7.5 Hz, Ar-H), 7.46 (1H, d, J 8.0 Hz, indolyl-H), 7.46 (1H, d, J 7.8 Hz, indolyl-H), 7.73 (1H, d, J 2.5 Hz, indolyl-H), 9.27 (1H, s, 8-NH), 11.64 (1H, s, indolyl-NH); d_C (100 MHz DMSO-d₆) 32.7, 56.0, 81.0, 85.9, 108.0, 111.5, 112.0, 119.7, 119.9, 121.5, 121.7, 121.8, 125.2, 127.4, 128.3, 129.3, 133.7, 135.9, 145.6, 154.5, 155.4, 161.5, 161.7; m/z (rel. int. %): 409 (11, M⁺), 303 (21), 302 (100), 260 (14); HRMS (ESI-QTOF (positive ionization): MH⁺ found 410.1720. C₂₃H₁₉N₇O requires 410.1724.

4.2.14. 2,4-Diamino-7-(1H-indol-3-yl)-5-(pyridin-4-yl)-5,8-dihydropyrido[2,3-d]pyrimidine-6-carbonitrile (**4n**)

Light yellow solid; [Found: C, 66.3; H, 4.3; N, 29.4. C₂₁H₁₆N₈ requires C, 66.3; H, 4.2; N, 29.5%]; Yield: 78%; m.p. 260–264 °C; IR (KBr, cm⁻¹): 3415, 3398, 3343 (NH, NH₂), 2187 (C≡N), 1621 (C=N); d_H (400 MHz, DMSO-d₆) 4.88 (1H, s, H-5), 5.80 (2H, s, 2-NH₂), 6.13 (2H, s, 4-NH₂), 7.09 (1H, t, J 7.6 Hz, indolyl-H), 7.17 (1H, t, J 7.5 Hz, indolyl-H), 7.37 (2H, d, J 5.2 Hz, Ar-H), 7.42 (1H, d, J 7.9 Hz, indolyl-H), 7.46 (1H, d, J 8.1 Hz, indolyl-H), 7.76 (1H, d, J 2.5 Hz, indolyl-H), 8.55 (2H, d, J 5.2 Hz, Ar-H), 9.49 (1H, s, 8-NH), 11.70 (1H, s, indolyl-NH); d_C (100 MHz DMSO-d₆) 37.9, 79.5, 84.2, 107.6, 112.1, 119.8, 121.6, 121.9, 122.2, 125.0, 127.9, 127.9, 136.0, 146.1, 149.9, 154.8, 162.0, 162.0; m/z (rel. int. %): 380 (4, M⁺), 303 (22), 302 (100), 260 (15); HRMS (ESI-QTOF positive ionization): MH⁺ found 381.1567. C₂₁H₁₆N₈ requires 381.1571.

4.2.15. 2,4-Diamino-7-(1H-indol-3-yl)-5-(pyridin-3-yl)-5,8-dihydropyrido[2,3-d]pyrimidine-6-carbonitrile (**4o**)

Light yellow solid; [Found: C, 66.4; H, 4.3; N, 29.5. C₂₁H₁₆N₈ requires C, 66.3; H, 4.2; N, 29.5%]; Yield: 87%; mp 253–258 °C; IR (KBr, cm⁻¹): 3507, 3437, 3387, 3319, 3215 (NH, NH₂), 2189 (C≡N),

1652 (C=N); d_H (400 MHz, DMSO- d_6) 4.86 (1H, s, H-5), 5.78 (2H, s, 2-NH₂), 6.12 (2H, s, 4-NH₂), 7.08 (1H, t, J 7.4 Hz, indolyl-H), 7.17 (1H, t, J 7.4 Hz, indolyl-H), 7.39 (1H, d, J 7.9 Hz, Ar-H), 7.41 (1H, d, J 7.9 Hz, indolyl-H), 7.46 (1H, d, J 8.1 Hz, indolyl-H), 7.71 (1H, d, J 8.0 Hz, Ar-H), 7.76 (1H, d, J 2.5 Hz, indolyl-H), 8.46 (1H, d, J 4.7 Hz, Ar-H), 8.64 (1H, d, J 2.1 Hz, Ar-H), 9.45 (1H, s, 8-NH), 11.68 (1H, s, indolyl-NH); d_C (100 MHz DMSO- d_6) 36.2, 80.4, 84.7, 107.6, 112.1, 119.8, 119.8, 121.6, 121.9, 123.9, 125.0, 127.8, 134.4, 135.9, 141.0, 145.7, 148.1, 148.2, 154.6, 161.9, 161.9; m/z (rel. int. %): 380 (5, M⁺), 303 (27), 302 (100), 260 (15); HRMS (ESI-QTOF positive ionization): MH⁺ found 381.1570. C₂₁H₁₆N₈ 381.1571.

4.2.16. 2,4-Diamino-7-(1H-indol-3-yl)-5-(pyridin-2-yl)-5,8-dihydropyrido[2,3-d]pyrimidine-6-carbonitrile (**4p**)

Light green solid; [Found: C, 66.4; H, 4.3; N, 29.5. C₂₁H₁₆N₈ requires C, 66.3; H, 4.2; N, 29.5%]; Yield: 76%; mp 230–233 °C; IR (KBr, cm⁻¹): 3359, 3171 (NH, NH₂), 2191 (C≡N), 1625 (C=N); d_H (400 MHz, DMSO- d_6) 4.88 (1H, s, H-5), 5.74 (2H, s, 2-NH₂), 6.10 (2H, s, 4-NH₂), 7.10 (1H, t, J 7.5 Hz, indolyl-H), 7.17 (1H, t, J 7.5 Hz, indolyl-H), 7.29 (1H, d, J 6.8 Hz, Ar-H), 7.46 (2H, d, J 7.8 Hz, indolyl-H), 7.50 (1H, d, J 7.7 Hz, Ar-H), 7.77 (1H, d, J 2.3 Hz, indolyl-H), 7.85 (1H, t, J 7.7 Hz, Ar-H), 8.53 (1H, d, J 4.2 Hz, Ar-H), 9.34 (1H, s, 8-NH), 11.68 (1H, s, indolyl-NH); d_C (100 MHz DMSO- d_6) 42.1, 79.2, 85.1, 107.9, 112.0, 119.7, 120.0, 121.7, 121.9, 122.2, 125.1, 127.6, 135.9, 137.5, 146.3, 148.8, 154.3, 161.8, 162.3, 163.5; m/z (rel. int. %): 380 (9, M⁺), 303 (24), 302 (100), 260 (15); HRMS (ESI-QTOF (positive ionization) MH⁺ found 381.1567. C₂₁H₁₆N₈ requires 381.1571.

4.2.17. 2,4-Diamino-5-(furan-2-yl)-7-(1H-indol-3-yl)-5,8-dihydropyrido[2,3-d]pyrimidine-6-carbonitrile (**4q**)

Yellow solid; [Found C, 65.1; H, 4.0; N, 26.5. C₂₀H₁₅N₇O requires C, 65.0; H, 4.1; N, 26.5%]; Yield: 70%; mp > 300 °C; IR (KBr, cm⁻¹): 3489, 3410, 3389, 3291, 3127 (NH, NH₂), 2194 (C≡N), 1629 (C=N); d_H (400 MHz, DMSO- d_6) 5.00 (1H, s, H-5), 5.74 (2H, s, 2-NH₂), 6.17 (2H, s, 4-NH₂), 6.22 (1H, s, Ar-H); 6.39 (1H, s, Ar-H); 7.11 (1H, t, J 7.6 Hz, indolyl-H), 7.18 (1H, t, J 7.5 Hz, indolyl-H), 7.48 (2H, t, J 8.0 Hz, indolyl-H), 7.58 (1H, s, Ar-H); 7.77 (1H, s, indolyl-H), 9.37 (1H, s, 8-NH), 11.69 (1H, s, indolyl-NH); d_C (100 MHz DMSO- d_6) 32.7, 77.1, 82.9, 105.3, 107.8, 110.3, 112.1, 119.8, 119.9, 121.7, 121.9, 125.1, 127.8, 136.0, 142.2, 146.3, 154.8, 156.3, 161.8, 162.0; m/z (rel. int. %): 369 (74, M⁺), 303 (27), 302 (100), 260 (24); HRMS (ESI-QTOF (positive ionization) MH⁺ found 370.1407. C₂₀H₁₅N₇O requires 370.1411.

4.2.18. (E)-3-(2,6-dichlorophenyl)-2-(1H-indole-3-carbonyl)acrylonitrile (**5r**)

Yellow solid; [Found C, 63.4; H, 2.9; N, 8.2. C₁₈H₁₀Cl₂N₂O requires C, 63.4; H, 3.0; N, 8.2%]; Yield: 72%; mp. 279–285 °C; IR (KBr, cm⁻¹): 3299 (NH), 2228 (C≡N), 1607 (C=O), 1581 (C=C); d_H (400 MHz, DMSO- d_6) 7.32 (2H, m, indolyl-H), 7.53–7.60 (2H, m, Ar-H + indolyl-H), 7.68 (2H, d, J 8.0 Hz, Ar-H), 8.22 (1H, d, J 7.6 Hz, indolyl-H), 8.25 (1H, s, indolyl-H), 8.35 (1H, s, C=H), 12.38 (1H, s, indolyl-NH); d_C (100 MHz DMSO- d_6) 112.7, 113.3, 115.2, 121.2, 121.3, 122.8, 123.9, 125.8, 128.7, 131.3, 132.1, 133.0, 136.4, 136.9, 147.9, 179.6; m/z (rel. int. %): 346 (5, M⁺), 340 (8), 305 (10), 144 (100).

4.2.19. (E)-3-(anthracen-9-yl)-2-(1H-indole-3-carbonyl)acrylonitrile (**5s**)

Yellow solid; [Found C, 83.9; H, 4.4; N, 7.5. C₂₆H₁₆N₂O requires C, 83.9; H, 4.3; N, 7.5%]; Yield: 81%; mp 298–301 °C; IR (KBr, cm⁻¹): 3356 (NH), 2223 (C≡N), 1631(C=O), 1574 (C=C); d_H (400 MHz, DMSO- d_6) 7.34–7.36 (2H, m, indolyl-H), 7.62–7.68 (5H, m, 4H Ar-H + indolyl-H), 8.15 (2H, d, J 8.4 Hz, Ar-H), 8.21 (2H, d, J 8.0 Hz, Ar-

H), 8.35 (1H, t, indolyl-H), 8.63 (1H, s, Ar-H), 8.81 (1H, s, indolyl-H), 9.20 (1H, s, C=H), 12.36 (1H, s, indolyl-NH); d_C (100 MHz DMSO- d_6) 112.6, 113.6, 116.3, 121.4, 121.5, 122.6, 123.7, 125.1, 125.8, 126.2, 126.8, 127.2, 128.4, 129.0, 129.5, 130.7, 136.1, 136.8, 152.0, 180.0; m/z (rel. int. %): 372 (13, M⁺), 227 (11), 144 (100), 89 (20).

4.3. Binding assays

Binding experiments were performed on striatal membranes. Each striatum was homogenized in 2 mL ice-cold Tris-HCl buffer (50 mM, pH = 7.4 at 22 °C) with a Polytron (4 s, maximal scale) and immediately diluted with Tris buffer. The homogenate was centrifuged either twice ([³H] SCH 23390 binding experiments) or four times ([³H] raclopride binding experiments) at 20,000 g for 10 min at 4 °C with resuspension in the same volume of Tris buffer between centrifugations. For [³H] SCH 23390 binding experiments, the final pellet was resuspended in Tris buffer containing 5 mM MgSO₄, 0.5 mM EDTA and 0.02% ascorbic acid (Tris-Mg buffer), and the suspension was briefly sonicated and diluted to a protein concentration of 1 mg/mL. An aliquot of 100 μL of freshly prepared membrane suspension (100 μg of striatal protein) was incubated for 1 h at 25 °C with 100 μL Tris buffer containing [³H] SCH 23390 (0.25 nM final concentration) and 800 μL of Tris-Mg buffer containing the required drugs. Non-specific binding was determined in the presence of 30 μM SK&F 38393 and represented around 2–3% of total binding. For [³H] raclopride binding experiments, the final pellet was resuspended in Tris buffer containing 120 mM NaCl, 5 mM KCl, 1 mM CaCl₂, 1 mM MgCl₂, and 0.1% ascorbic acid (Tris-ions buffer), and the suspension was treated as described above. A 200 μL aliquot of freshly prepared membrane suspension (200 μg of striatal protein) was incubated for 1 h at 25 °C with 200 μL of Tris buffer containing [³H] raclopride (0.5 nM final concentration) and 400 μL of Tris-ions buffer containing the drug being investigated. Non-specific binding was determined in the presence of 50 μM apomorphine and represented around 5–7% of total binding. In both cases, incubations were stopped by addition of 3 mL of ice cold buffer (Tris-Mg buffer or Tris-ions buffer, as appropriate) followed by rapid filtration through Whatman GF/B filters using a Brandel harvester (model M – 24, Biochemical Research and Development Laboratories, Inc.). Tubes were rinsed with 3 mL ice cold buffer, and filters were washed with 3 × 3 mL ice-cold buffer. After the filters had been dried, radioactivity was counted in 4 mL scintillation liquid (Optiphase “Hisafe” 2, Perkin Elmer). Filter blanks corresponded to approximately 0.5% of total binding and were not modified by drugs.

4.4. Computational details

4.4.1. Molecular docking and molecular dynamics approach

3D models of the human D1DR and D2DR were used for the molecular modeling study. The D1DR model is based on the homology model from the crystallized D2DR, D3DR, β₂-adrenoceptor, and A_{2α} adenosine receptor as templates. In the case of D2DR we have used the one that has been recently crystallized (PDB code: 6CM4) [73].

Molecular docking simulations were performed using the AutoDockVina software [77]. Several docking poses were considered and complexes with the lowest docking-energy according to the standard scoring function was regarded as the most favorable orientation and then used for MD calculations. Previously reported experimental evidence was taken into account to judge the validity of the docking poses.

Antechamber Software in the AmberTools package was used to generate the parameters for MD simulations considering FF99SB

[78] and GAFF [79] force fields. All MD simulations were performed with the Amber 16 software package [80] (All-atoms force field FF99SB) using periodic boundary conditions for constant volume and cubic simulation cells. The particle mesh Ewald method (PME) was applied using a grid spacing of 1.2 Å, a spline interpolation order of 4 and a real space direct sum cutoff of 10 Å. The SHAKE algorithm was applied allowing for an integration time step of 2 fs. MD simulations were carried out at 310 K temperature. Three MD simulations of 10 ns were conducted for each system under different starting velocity distribution functions; thus, in total 30 ns were simulated for each complex. The NPT ensemble was employed using Berendsen coupling to a baro/thermostat (target pressure 1 atm, relaxation time 0.1 ps). Post MD analysis was carried out with program PTRAJ.

Acknowledgments

The authors gratefully acknowledge the Departamento Administrativo de Ciencia, Tecnología e Innovación (COLCIENCIAS), Consejería de Economía, Innovación, Ciencia y Empleo (Junta de Andalucía, Spain) and Universidad de Jaén for financial support. D.F.V. thanks COLCIENCIAS for his young researcher grant 617 - 2013. The authors R.D.T, S.A.A and R.D.E gratefully acknowledge grants from Universidad Nacional de San Luis (UNSL-Argentina) and Consejo Nacional de Investigaciones Científicas y Técnicas (CONICET-Argentina) partially supported this work. The authors also thank 'Centro de Instrumentación Científico-Técnica de Universidad de Jaén' for data collection.

Appendix A. Supplementary data

Supplementary data to this article can be found online at <https://doi.org/10.1016/j.tet.2018.10.038>.

References

- [1] S. Bräse, *Privileged Scaffolds in Medicinal Chemistry*, Royal Society of Chemistry, Cambridge, UK, 2015.
- [2] E. Vitaku, D.T. Smith, J.T. Njardarson, *J. Med. Chem.* 57 (2014) 10257–10274.
- [3] A. Agarwal, R. Ashutosh, N. Goyal, P.M.S. Chauhan, S. Gupta, *Bioorg. Med. Chem.* 13 (24) (2005) 6678–6684.
- [4] S.N. Mokale, S.S. Shinde, R.D. Elgire, J.N. Sangshetti, D.B. Shinde, *Bioorg. Med. Chem. Lett.* 20 (15) (2010) 4424–4426.
- [5] J. Quiroga, C. Cisneros, B. Insuasty, R. Abonía, C. Cruz, M. Nogueras, J.M. De la Torre, M. Sortino, S. Zacchino, *J. Heterocycl. Chem.* 43 (2006) 299–306.
- [6] J.-J., Liu, K.-C., Luk, 5,8-dihydro-6H-pyrido[2,3-d]pyrimidin-7-ones. *US Patent 7098332(B2)*, August 29, 2006 (CAN 141:71554) ..
- [7] C. Zhang, G. Sun, Q. Peng, S. Zhu, D. Ni, *RSC Adv.* 6 (2016) 73953–73958.
- [8] D. Insuasty, R. Abonía, B. Insuasty, J. Quiroga, K.K. Laali, M. Nogueras, J. Cobo, *ACS Comb. Sci.* 19 (8) (2017) 555–563.
- [9] P.J. Zhang, J. Huang, C. Liu, X.-F. Lu, B.-X. Wu, L. Zhao, N. Lu, Q.-L. Guo, Z.-Y. Li, C. Jiang, *Chin. Chem. Lett.* 25 (2014) 1025–1028.
- [10] C. Zhang, G. Sun, Q. Peng, S. Zhu, D. Ni, *RSC Adv.* 6 (2016) 73953–73958.
- [11] M.M. Gineinah, M.N.A. Nasr, S.M.I. Badr, W.M. El-Husseiny, *Med. Chem. Res.* 22 (2013) 3943–3952.
- [12] F. Buron, J.Y. Mérour, M. Akssira, G. Guillaumet, S. Routier, *Eur. J. Med. Chem.* 95 (2015) 76–95.
- [13] (a) A.R. Bhat, R.S. Dongrea, G.A. Naikoo, I.U. Hassanb, T.J. Ara, *Taibah Univ. Sci.* 11 (2017) 1047–1069; (b) M. Mamaghani, R.H. Nia, *J. Heterocycl. Chem.* 54 (2017) 1700–1722.
- [14] D. Insuasty, R. Abonía, B. Insuasty, J. Quiroga, K.K. Laali, M. Nogueras, J. Cobo, *ACS Comb. Sci.* 19 (2017) 555–563.
- [15] F. Shi, J. Ding, S. Zhang, W.J. Hao, C. Cheng, S. Tu, *Bioorg. Med. Chem. Lett.* 21 (2011) 1554–1558.
- [16] S. Tu, J. Zhang, X. Zhu, J. Xu, Y. Zhang, Q. Wang, R. Jia, B. Jiang, J. Zhang, *Bioorg. Med. Chem. Lett.* 16 (2006) 3578–3581.
- [17] J. Quiroga, J. Trilleras, A. Sánchez, B. Insuasty, R. Abonía, M. Nogueras, J. Cobo, *Let. Org. Chem.* 6 (2009) 381–383.
- [18] J. Quiroga, C. Cisneros, B. Insuasty, R. Abonía, M. Nogueras, A. Sánchez, *Tetrahedron Lett.* 42 (2001) 5625–5627.
- [19] J. Quiroga, C. Cisneros, B. Insuasty, R. Abonía, S. Cruz, M. Nogueras, J.M. De la Torre, M. Sortino, S. Zacchino, *J. Heterocycl. Chem.* 43 (2006) 299–306.
- [20] J. Rangel, C. Díaz-Urbe, A. Rodríguez-Serrano, X. Zarate, Y. Serge, W. Vallejo, M. Nogueras, J. Trilleras, J. Quiroga, J. Tatchen, J. Cobo, *J. Mol. Struct.* 1137 (2017) 431–439.
- [21] Y. Wang, L. Zhou, Y. Zhu, M. Zhang, L. Song, H. Deng, *J. Fluor. Chem.* 200 (2017) 162–168.
- [22] A. Upadhyay, L.K. Sharma, V.K. Singh, R.K.P. Singh, *Tetrahedron Lett.* 57 (2016) 5599–5604.
- [23] Y. Dommaraju, S. Bora, D. Prajapati, *Org. Biomol. Chem.* 13 (2015) 9181–9185.
- [24] S. Abdolmohammadi, M. Afsharpour, *Chin. Chem. Lett.* 23 (2012) 257–260.
- [25] S. Chand, S.S. Sandhu, J.S. Sandhu, *Indian J. Chem.* 53 (2014) 728–732.
- [26] P.S. Naidu, P. Borah, P.J. Bhuyan, *Tetrahedron Lett.* 53 (2012) 4015–4017.
- [27] F. Nemat, R. Saedirad, *Chin. Chem. Lett.* 24 (2013) 370–372.
- [28] S. Karabulut, N. Sizochenko, A. Orhan, J. Leszczynski, *J. Mol. Graph. Model.* 70 (2016) 23–29.
- [29] A. Gangjee, O.A. Namjoshi, S. Raghavan, S.F. Queener, R.L. Kisiulik, V. Cody, *J. Med. Chem.* 56 (2013) 4422–4441.
- [30] A. Gangjee, O.O. Adair, M. Pagley, S.F. Queener, *J. Med. Chem.* 51 (2008) 6195–6200.
- [31] A. Gangjee, O.O. Adair, S.F. Queener, *J. Med. Chem.* 46 (2003) 5074–5082.
- [32] A. Gangjee, Y. Zeng, J. McGuire, R.L. Kisiulik, *J. Med. Chem.* 45 (2002) 5173–5181.
- [33] A. Gangjee, A. Vasudevan, S.F. Queener, R.L. Kisiulik, *J. Med. Chem.* 39 (1996) 1438–1446.
- [34] M. Font, A. González, J.A. Palop, C. Sanmartín, *Eur. J. Med. Chem.* 46 (2011) 3887–3899.
- [35] M. Zink, H. Lanig, R. Troschütz, *Eur. J. Med. Chem.* 39 (2004) 1079–1088.
- [36] R.D. Tosso, S.A. Andújar, L. Gutiérrez, E. Angelina, R. Rodríguez, M. Nogueras, H. Baldoni, F.D. Suvire, J. Cobo, R.D. Enriz, *J. Chem. Inf. Model.* 53 (2013) 2018–2032.
- [37] J.C. Garro Martínez, M.F. Andrada, E.G. Vega-Hissi, F.M. Garibotto, M. Nogueras, R. Rodríguez, J. Cobo, R.D. Enriz, M.R. Estrada, *Med. Chem. Res.* 26 (2016) 247–261.
- [38] R.D. Tosso, M. Vettorazzi, S.A. Andújar, L.J. Gutiérrez, J.C. Garro, E. Angelina, R. Rodríguez, F.D. Suvire, M. Nogueras, J. Cobo, R.D. Enriz, *J. Mol. Struct.* 1134 (2017) 464–474.
- [39] L.J. Gutiérrez, O. Parravicini, E. Sánchez, R. Rodríguez, J. Cobo, R.D. Enriz, *J. Biomol. Struct. Dyn.* (2018). <https://doi.org/10.1080/07391102.2018.1424036>.
- [40] T. Govender, G. Maguire, H. Kruger, M. Shiri, *Curr. Org. Synth.* 10 (2013) 737–750.
- [41] A. El-Mekabaty, A. Mesbah, A.A. Fadda, *J. Heterocycl. Chem.* 54 (2017) 916–922.
- [42] T. Chen, X.P. Xu, H.F. Liu, S.J. Ji, *Tetrahedron* 67 (2011) 5469–5476.
- [43] J. Wang, H. Liu, R. Wen, Z. Zhu, J. Li, S. Zhu, *Res. Chem. Intermed.* 43 (2017) 4575–4583.
- [44] M. Gompel, M. Leost, E.B. De Kier Joffe, L. Puricelli, L.H. Franco, J. Palermo, L. Meijer, *Bioorg. Med. Chem. Lett.* 14 (2004) 1703–1707.
- [45] A.E. Wright, S.A. Pomponi, S.S. Cross, P. McCarthy, *J. Org. Chem.* 57 (1992) 4772–4775.
- [46] B. Jiang, J.M. Smallheer, C. Amaral-Ly, M.A. Wuonola, *J. Org. Chem.* 59 (1994) 6823–6827.
- [47] S. Sakemi, H.H. Sun, *J. Org. Chem.* 56 (1991) 4304–4307.
- [48] T. Heinrich, H. Böttcher, G.D. Bartoszyk, H.E. Greiner, C.A. Seyfried, C. Van Amsterdam, *J. Med. Chem.* 47 (2004) 4677–4683.
- [49] T. Heinrich, H. Böttcher, R. Gericke, G.D. Bartoszyk, S. Anzali, C.A. Seyfried, H.E. Greiner, C. Van Amsterdam, *J. Med. Chem.* 47 (2004) 4684–4692.
- [50] R. Puig de la Bellacasa, G. Roué, P. Balsas, P. Pérez-Galán, J. Teixidó, D. Colomer, J.I. Borrell, *Eur. J. Med. Chem.* 86 (2014) 664–675.
- [51] A.A. Joshi, S.S. Narkhede, C.L. Viswanathan, *Bioorg. Med. Chem. Lett.* 15 (2005) 73–76.
- [52] A.W.-H. Cheung, B. Banner, J. Bose, K. Kim, S. Li, N. Marcopulos, L. Orzechowski, J.A. Sergi, K.C. Thakkar, B.-B. Wang, W. Yun, C. Zwingelstein, S. Berthel, A.R. Olivier, *Bioorg. Med. Chem. Lett.* 22 (2012) 7518–7522.
- [53] M.J. Lavecchia, R. Puig De La Bellacasa, J.I. Borrell, C.N. Cavasotto, *Bioorg. Med. Chem.* 24 (2016) 768–778.
- [54] Y. Chen, J.G. Moloney, K.E. Christensen, M.G. Moloney, *Antibiotics* 6 (2) (2017) 2.
- [55] I. Berenguer, N. El Aouad, S.A. Andújar, V. Romero, F. Suvire, T. Freret, A. Bermejo, M.D. Ivorra, R.D. Enriz, M. Boulouard, N. Cabedo, D. Cortés, *Bioorg. Med. Chem.* 17 (2009) 4968–4980.
- [56] N. El Aouad, I. Berenguer, V. Romero, P. Marín, A. Serrano, S.A. Andújar, F. Suvire, A. Bermejo, M.D. Ivorra, R.D. Enriz, N. Cabedo, D. Cortés, *Eur. J. Med. Chem.* 40 (2009) 4616–4621.
- [57] S.A. Andújar, F. Suvire, I. Berenguer, N. Cabedo, P. Marín, L. Moreno, M.D. Ivorra, D. Cortés, R.D. Enriz, *J. Mol. Model.* 18 (2011) 419–431.
- [58] J. Párraga, N. Cabedo, S.A. Andújar, L. Piqueras, L. Moreno, A. Galán, E. Angelina, R.D. Enriz, M.D. Ivorra, M.J. Sanz, D. Cortés, *Eur. J. Med. Chem.* 68 (2013) 150–166.
- [59] J. Párraga, S.A. Andújar, S. Rojas, L. Gutiérrez, N. El Aouad, M. Sanz, R.D. Enriz, N. Cabedo, D. Cortés, *Eur. J. Med. Chem.* 122 (2016) 27–42.
- [60] O. Parravicini, M.L. Bogado, S. Rojas, E.L. Angelina, S.A. Andújar, L.J. Gutiérrez, N. Cabedo, M.J. Sanz, M.-P. López-Gresa, D. Cortés, R.D. Enriz, *J. Mol. Model.* 23 (2017) 273.
- [61] N. Ye, J.L. Neumeyer, R.J. Baldessarini, X. Zhen, A. Zhang, *Chem. Rev.* 113 (5) (2013) PR123–PR178.
- [62] J.M. Beaulieu, R.R. Gainetdinov, *Pharmacol. Rev.* 63 (2011) 182–217.

- [63] M.M. Sarmah, D. Prajapati, W. Hub, *Synlett* 24 (2013) 471–474.
- [64] X. Berzosa, X. Bellatriu, J. Teixidó, J.I. Borrell, *J. Org. Chem.* 75 (2010) 487–490.
- [65] S. Tu, J. Zhang, R. Jia, B. Jiang, Y. Zhang, H. Jiang, *Org. Biomol. Chem.* 5 (2007) 1450–1453.
- [66] S. Tu, Q. Wang, J. Xu, X. Zhu, J. Zhang, B. Jiang, R. Jia, Y. Zhang, J. Zhang, *J. Heterocycl. Chem.* 43 (2006) 855–858.
- [67] A.M. Schoffstall, *J. Org. Chem.* 36 (16) (1971) 2385–2387.
- [68] D.A. Erlanson, W. Jahnke (Eds.), *Fragment-based Drug Discovery: Lessons and Outlook*, vol. 67, Wiley-VCH, 2016.
- [69] J.M. Khurana, A. Chaudhary, B. Nand, A. Lumb, *Tetrahedron Lett.* 53 (2012) 3018–3022.
- [70] Y. Ogiwara, K. Takahashi, T. Kitazawa, N. Sakai, *J. Org. Chem.* 80 (2015) 3101–3110.
- [71] N.V. Lakshmi, P. Thirumurugan, K.M. Noorulla, P.T. Perumal, *Bioorg. Med. Chem. Lett.* 20 (2010) 5054–5061.
- [72] P. Seetham Naidu, B. Pallabi, J.B. Pulak, *Tetrahedron Lett.* 53 (2012) 4015–4017.
- [73] S. Wang, T. Che, A. Levit, B.K. Shoichet, D. Wacker, B.L. Roth, *Nature* 555 (2018) 269–273.
- [74] S.A. Andújar, R.D. Tosso, D.D. Suvire, E. Angelina, N. Peruchena, N. Cabedo, D. Cortés, R.D. Enriz, *J. Chem. Inf. Model.* 52 (2012) 99–112.
- [75] W. Traube, *Ber. Dtsch. Chem. Ges.* 37 (1904) 4544–4547.
- [76] R.M. Abdel-Motaleb, A.-M.A.-S. Makhloof, H.M. Ibrahim, M.H. Elnagdi, *J. Heterocycl. Chem.* 44 (2007) 109–114.
- [77] G.M. Morris, R. Huey, W. Lindstrom, M.F. Sanner, R.K. Belew, D.S. Goodsell, A.J. Olson, *J. Comput. Chem.* 30 (2009) 2785–2791.
- [78] K. Lindorff-Larsen, S. Piana, K. Palmo, P. Maragakis, J.L. Klepeis, R.O. Dror, D.E. Shaw, *Proteins* 78 (2010) 1950–1958.
- [79] J. Wang, R.M. Wolf, J.W. Caldwell, P.A. Kollman, D.A. Case, *J. Comput. Chem.* 25 (2004) 1157–1174.
- [80] D.A. Case, R.M. Betz, D.S. Cerutti, T.E. Cheatham, T.A. Darden, R.E. Duke, T.J. Giese, H. Gohlke, A.W. Goetz, N. Homeyer, S. Izadi, P. Janowski, J. Kaus, A. Kovalenko, T.S. Lee, S. LeGrand, P. Li, C. Lin, T. Luchko, R. Luo, B. Madej, D. Mermelstein, K.M. Merz, G. Monard, H. Nguyen, H.T. Nguyen, I. Omelyan, A. Onufriev, D.R. Roe, A. Roitberg, C. Sagui, C.L. Simmerling, W.M. Botello-Smith, J. Swails, R.C. Walker, J. Wang, R.M. Wolf, X. Wu, L. Xiao, P.A. Kollman, *AMBER 2016*, University of California, San Francisco, 2016.